

Nanoscale

Accepted Manuscript



This is an *Accepted Manuscript*, which has been through the Royal Society of Chemistry peer review process and has been accepted for publication.

Accepted Manuscripts are published online shortly after acceptance, before technical editing, formatting and proof reading. Using this free service, authors can make their results available to the community, in citable form, before we publish the edited article. We will replace this *Accepted Manuscript* with the edited and formatted *Advance Article* as soon as it is available.

You can find more information about *Accepted Manuscripts* in the [Information for Authors](#).

Please note that technical editing may introduce minor changes to the text and/or graphics, which may alter content. The journal's standard [Terms & Conditions](#) and the [Ethical guidelines](#) still apply. In no event shall the Royal Society of Chemistry be held responsible for any errors or omissions in this *Accepted Manuscript* or any consequences arising from the use of any information it contains.

Title: Anderson Localization of light in a colloidal suspension (TiO₂@Silica)

Author(s): *Ernesto Jimenez-Villar^{1*}, Iran F. da Silva², Valdeci Mestre^{3, 4}, Paulo C. de Oliveira⁴, Wagner M. Faustino², Gilberto F. de Sá¹*

¹Departamento de Química Fundamental, Universidade Federal de Pernambuco, Recife, Pernambuco, 50670-901, Brazil

²Departamento de Química, Universidade Federal da Paraíba, João Pessoa, Paraíba 58051-970, Brazil

³CCEA, Universidade Estadual da Paraíba, Patos, Paraíba 58706-560, Brazil

⁴Departamento de Física, Universidade Federal da Paraíba, João Pessoa, Paraíba 58051-970, Brazil

E-mail: Ernesto.Jimenez@uv.es

Keywords: Localization of light, enhanced absorption, Photonics in disorder media, Core-shell nanoparticles.

Abstract: In recent years, there has been dramatic progress in the photonics field in disordered media, ranging from applications in solar collectors, photocatalyzers, random lasing, and other novel photonic functions, to investigations into fundamental topics, such as light confinement and other phenomena involving photon interactions. This paper reports several experimental evidences of localization transition in a strongly disordered scattering medium composed of a colloidal suspension of core-shell nanoparticles (TiO₂@Silica) in ethanol solution. We demonstrate the crossover from a diffusive transport to a localization transition regime as nanoparticles concentration is increased, and that an enhanced absorption effect arises at localization transition.

Introduction

Scattering media have attracted much attention in recent years, due to potential applications in solar energy, ^[1,2] photocatalyzers, ^[3] random lasers ^[4], and novel optical devices. ^[5,6] The coherent superposition of input fields could give rise to fundamental effects, such as light confinement (localization), ^[7,8,9,10,11] enhanced backscattering, ^[12] much further transmission than the mean free path through the sample, ^[13] and coherently enhanced absorption.

^[14]Localization of light and a wide variety of associated phenomena have greatly attracted the attention of researchers in the past decades. Localization in a three-dimensional (3D) system could only take place in extremely strongly scattering medium. The requirement is known as the Ioffe–Regel criterion ($kl_s \leq 1$),^[15] where $k = 2\pi/\lambda$ and l_s are the wave number and scattering mean free path, respectively. However, critical regime in the approaching to localization (localization transition) has been reported to not so high scattering strengths ($kl_s \leq 5$).^[9] In the localization regime, the transmission decreases exponentially instead of linearly with the thickness of a sample (d). At the transition, the transmission must have a quadratic dependence on the inverse thickness.^[16, 17] This quadratic decay can be interpreted as the onset of localization. However, the residual absorption can provoke a similar decay, which has led to an important debate.^[18, 19, 20] In fact, various evidences of Anderson localization have been reported, but questioned. Additionally, according to the theoretical prediction of Sajeev John, an enhanced absorption must arise when the system approaches to mobility edge.^[7] Recently, Sperling *et al.* provided evidence for the transition from diffusive light propagation to localization.^[10] Significantly, they employed approaches that are intrinsically independent of residual absorption. The localization or localization transition regimes are extremely difficult to be obtained, especially in a colloidal suspension. Particles in a suspension tend to agglomerate and/or precipitate, which causes a decrease in scattering strength. Indeed, to our knowledge, the localization or localization transition regimes have not yet been reported in a colloidal suspension. A scattering medium in liquid suspension, among others advantages, facilitates the dissolution of molecules, harvesting of products resulting from a photochemical reaction and allows a better study of the Anderson localization itself and associated phenomena. In previous works,^[21, 22] we introduced a scattering medium for a random laser composed of a colloidal suspension of core-shell TiO₂@Silica nanoparticles (Nps), whose silica shell showed an irregular morphology. The silica shell provides a better optical colloidal stability (OCS) and light-coupling enhancement (LCE) with TiO₂ scatter

cores. Moreover, the silica coatings provide inertness^[23,24] and high dispersibility of Nps,^[25, 26, 27] which has enabled their use in numerous applications.^[28, 29, 30] The effects of OCS and LCE were proposed as likely causes of the increased scattering strength.^[21, 22] I_s experimentally determined can be several times lower than I_s calculated by Mie-scattering calculation.^[22] This fact was explained through a possible light coupling enhancement effect with the TiO₂ cores, due to light refraction at ethanol-silica interface. Here, by using an improved Stöber method,^[31, 32] TiO₂ nanoparticles were coated with a homogenous silica shell of ~40 nm thickness. A homogeneous silica shell must improve the LCE effect, leading to a significant scattering strength, higher than the reported in our previous works.^[21, 22] Here, localization transition was demonstrated by several approaches, among others-measurement of the relative fluctuations of the inverse participation ratio (propagating experiment), inversely proportional to dimensionless conductance, which reflects the extent of localization, even in the presence of absorption.^[19] Additionally, an enhanced absorption phenomenon is reported at the localization transition. Localization of light in a colloidal suspension could open new avenues for the designing and manufacture of novel photochemical reactors, powerful sensing tools and others photonic devices based on highly disordered scattering media.

Material and Methods:

Synthesis and characterization of Silica shell:

In the first stage, 5 g of TiO₂Nps were dispersed in 500 ml of spectroscopic ethanol. The suspension of TiO₂ nanoparticles was placed in an ultrasound bath and 6.67 mL of ammonia and 10 mL of TEOS were added. The TEOS and commercial ammonia (NH₄OH 28%-30%) were added alternately in 100 portions of 100 μ l and 220 μ l, respectively. The synthesized TiO₂@Silica nanoparticle suspension was rota-evaporated and dried in an oven at 70 °C for 2 h. In order to prepare the scattering medium with different [Nps], the TiO₂@Silica powder is re-dispersed in the appropriate ethanol volume. The silica coating on the TiO₂ nanoparticles

was examined by transmission electron microscopy (TEM) and electron-energy-loss spectroscopy (EELS), using a Carl Zeiss Libra 120 kV transmission electron microscope. The stoichiometric ratio (Ti/Si) of nanoparticles (TiO₂@Silica) was determined by Energy Dispersive X-Ray fluorescence (ED-XRF). The mass percentage ratio (Ti/Si), determined by ED-XRF, was Ti₇₂/Si₂₈. Considering the typical density of the silica obtained by the TEOS hydrolysis around 2 g cm⁻³,^[33] we determined an average silica shell thickness of ~42 nm. The sample preparation details for these characterizations and additional TEM images can be found in the supplementary information.

Transport experiments:

For transport experiments, the second harmonic of a *Q*-switched Nd: YAG Continuum Minilite II (25 mJ, 532 nm, pulse width of ~4ns, repetition rate up to 15 Hz, multimode, linearly polarized and spot size of 3 mm) was used and attenuated 10³ times by neutral density filters (1μJ)(see supplementary information, Figure S2a and S2b, for experimental setups). For transmission coefficient measurements, a CW He-Ne laser, model Uniphase 1125P (10 mW, 633 nm) was also used. The transmission coefficient ($T(d)$) is defined as the ratio between total transmitted flux and the incident flux. The total transmission is measured with an integrating sphere placed in contact with the back of the sample (fused silica cuvette). For the propagation experiments and coherent backscattering, the same CW He-Ne laser was used (experimental setups, Figure S4 and S5a, supplementary information).

Result and discussion

Silica shell study

Figure 1 shows the TEM image and mapping EELS (Si) of the core-shell TiO₂@Silica NPs. In the TEM image (Figure 1a), the silica coating on the TiO₂ particles shows a regular morphology, with a thickness around 40 nm. Figure 1b shows the Si mapping EELS (orange) of TiO₂@Silica Nps. As it is observed, the silica coating presents great homogeneity. A homogeneous silica shell is expected to improve the LCE effect, leading to increased

scattering strength. A better definition of the ethanol-silica interface should increase the light refracted toward the TiO₂ scatter core.

Scattering Medium Study

In order to study the scattering medium composed of these core-shell nanoparticles (TiO₂@Silica) in ethanol solution, a set of transport experiments were performed. The transmitted coherent intensity (I_{TC}) and the transmission coefficient ($T(d)$) were determined as a function of slab thickness (d) for [Nps] of 280, 140, 70, 47, and 14; $\times 10^{10}$ Nps ml⁻¹. I_{TC} should show an exponential decay (linear in log scale). The l_s values can be determined from slopes. Figure 2a shows the coherent transmission curve (normalized) versus slab thickness for [140 $\times 10^{10}$ Nps ml⁻¹], using the Nd:Yag laser. Three different parts can be distinguished (I, II, and III). In part I, the transmitted intensity decreases more quickly than an exponential. The green line represents the exponential decay ($I_{TC} = e^{-d/l_s}$) determined by fitting with the first experimental points. From the derivative, an initial (d near to zero) scattering mean free path (l_{s0}) is obtained, $l_{s0} = 1.15\mu\text{m}$. The red line represents the decay behavior of experimental points. As can be observed, the slope is not constant; it progressively decreases as slab thickness is increased (part I). For slab thickness greater than $\sim 6\mu\text{m}$ (near point A), the transmitted intensity starts to decay more slowly. This should be because the diffuse intensity (I_{dif}) starts to overweigh the coherent intensity. Near point B, the inelastic scattering should start to play a role, and in part III, the decay is exponential ($e^{-d/l_{MA}}$, blue line). From the inverse slope, we can obtain the macroscopic “absorption” length (l_{MA}), where “absorption” represents the losses by inelastic scattering processes. l_{MA} can be expressed as $l_{MA} = (l_T \times l_{in})^{1/2}$, where l_T and l_{in} are the transport and inelastic mean free path, respectively. l_T for d near to zero (l_{T0}), can be determined from the l_{s0} values by $l_{T0} = \frac{l_{s0}}{1-\langle \cos \theta \rangle}$ equation, where $\langle \cos \theta \rangle$ is the average cosine of the scattering angle (see sup. Information). l_{in} near to zero (

l_{In0}), determined through above equation ($l_{In0} \approx 2680 \mu m$), is more than three orders larger than $l_{s0} = 1.15 \mu m$ and more than 10 times larger than the average photon path length ($l_{eO(Micro)}$) inside the scattering medium before being reflected ($l_{eO(Micro)} \approx 240 \mu m$).^[34] At localization transition, $l_{eO(Micro)}$ must be approximately equal or lightly higher than the optical path length of localized photons inside the scattering medium (microscopic coherence length, ξ_{coh}), since the overall pathlength of non localized photons must vanish when l_T decreases approaching to localization.

Figure 2b shows the coherent transmission curves (part I) for [Nps] of 140, 70, 47 and $14 \times 10^{10} \text{ Nps ml}^{-1}$. The transmitted intensity decreases more quickly than an exponential for $[\text{Nps}] \geq 47 \times 10^{10} \text{ Nps ml}^{-1}$. This effect is pronounced as [Nps] is increased (from 47 to $140 \times 10^{10} \text{ Nps ml}^{-1}$). This fact represents an anomalous behavior. The green lines represent the exponential decay, determined by fitting with the first experimental points, and red lines represent the experimental behavior. For $[280 \times 10^{10} \text{ Np ml}^{-1}]$, the intensity in part I decays extremely quickly, which prevented a reliable measurement. For $[14 \times 10^{10} \text{ Nps ml}^{-1}]$, I_{TC} decay exponentially. l_{s0} values extracted from the derivative of the green lines are plotted as a function of [Nps] (Figure 2c), revealing that l_{s0} decrease linearly as [Nps] is increased ($l_{s0} \propto 1/[\text{Nps}]$).

Part III of the coherent transmission curves are shown in the supporting information (fig. S2 c-g). l_{MA} determined from the inverse slopes (parts III) shows an anomalous behavior as [Nps] is increased. $(l_{MA})^{-1}$ increases more quickly than the expected linear increase (fig. S2h supp. information). Notice that, if l_{T0} and l_{In0} would be inversely proportional to [Nps], a $(l_{MA})^{-1} \propto [\text{Nps}]$ dependence must be expected. Therefore, in order to study in depth this anomalous “absorption” behavior, l_{In0} values were determined through $l_{MA} = (l_{T0} \times l_{In0})^{1/2}$ equation (table SI supp. information). $(l_{In0})^{-1}$ per filling fraction (α_{FF0}) is plotted (fig. 2d left) as a function of the filling fraction ([FF]). For each [FF], α_{FF0} values (“absorption” coefficient) are

determined from $\alpha_{FF0} = (l_{In0} \times [FF])^{-1}$. In order to determinate l_{In0} for $[280 \times 10^{10} \text{ Np ml}^{-1}]$, l_{T0} was extrapolated following the $l_{T0} \propto 1/[N_{ps}]$ criterion. Contrary to expectations, α_{FF0} is not constant; it increases quickly in $[FF]$ as a function $\alpha_{FF0} = \alpha_0 + C([FF] - [FF_0])^2$, where C is a constant, and α_0 and $[FF_0]$ are α_{FF0} at the limit of diffusive regime and the critical filling fraction which starts the α_{FF0} anomalous increase, respectively. This anomalous increase of “absorption” coefficient at d near to zero represents a very interesting result, which could be strong evidence of the existence of the photon mobility edge.^[7, 35, 36] According to the theoretical prediction of Sajeev John, a signature of the electromagnetic mobility edge in a disordered medium is an anomalous rise in energy absorption.^[7] Fig. 2d (right) shows the enhanced “absorption” factor for d near to zero (γ_0) determined by the ratio between effective and classical “absorption” ($\gamma_0 = \alpha_{FF0}/\alpha_0$). This γ_0 parameter could be interpreted such that one photon travels an average of γ_0 times around a closed loop path at d near to zero, i.e. each photon would interact an average of γ_0 times with the same particles, atoms or molecules within the closed loop paths. This idea could be extrapolated to the elastic polarization of valence electrons to virtual states, which would imply an increase also in the effective refractive index at d near to zero (n_{eff0}). This supposed increase of the effective refractive index by localization effect finds a parallel in the dynamic barrier proposed by Campagnano and Nazarov^[37] in the border of a disordered electronic medium at localization.

Figure 2e shows the transmission coefficients, measured using two laser sources: one pulsed (Nd:Yag, 532nm) and the other CW (He-Ne, 633nm), for $[N_{ps}]$ of 280, 140, 70, 47 and 14; $\times 10^{10} \text{ Nps ml}^{-1}$. The fluence of the Nd:Yag laser was $\sim 10^7$ times higher than of He-Ne laser. For $[N_{ps}] \geq 47 \times 10^{10} \text{ Nps ml}^{-1}$, the transmission coefficient shows a similar quadratic decay $T(d) \propto \beta(d_0 + d)^{-2}$ for the two laser sources, which suggests a quadratic decay seemingly insensitive to wavelength and fluence (in this range). This is exactly the behavior of the scaling theory of localization at the localization transition, predicted by Anderson and

co-workers.^[16,17] For $14 \times 10^{10} \text{Nps ml}^{-1}$, the transmission coefficient shows a classical behavior $(d_0 + d)^{-1}$. The green and red solid lines (Figure 2e) are the fitting with experimental points for Nd:Yag and He-Ne lasers, respectively. Notice that for $[\text{Nps}] \leq 140 \times 10^{10} \text{Nps ml}^{-1}$, the transmission coefficients tend to $\sim(0.47)$ instead of 1. This effect is explained by the total internal reflection at the output interface air-silica of cuvette (see supporting information for an expanded discussion). For $[280 \times 10^{10} \text{Nps ml}^{-1}]$, the transmission coefficient tends to ~ 0.3 instead of expected value (~ 0.42), which must be a result of an appreciable increase of the losses due to enhanced “absorption”. Notice that, appreciable losses in the light transport must lead to a transmission coefficient lower than expected, especially at $d=0$. From the quadratic decay of the total transmission, it is difficult to demonstrate being so close to the localization transition, since the losses by the inelastic scattering processes could lead to a similar decay.^[18] However, a detailed treatment of the data and an expanded discussion about “absorption” contribution can be found in the supporting information.

From the above results it could be inferred that an anomalous light transport is reached for $[\text{Nps}] \geq 47 \times 10^{10} \text{Nps ml}^{-1}$. However, l_{T0} values seem too high, corresponding to $kl_{T0} > 5$. In order to resolve this mismatch, l_T values were also determined by backscattering method (supp. Information, fig. S5). l_T values, extracted from the angle of backscattering cones for $[47, 70, 140 \text{ and } 280; \times 10^{10} \text{Nps ml}^{-1}]$, correspond to $0.93, 0.7, 0.64$ and $0.47 \mu\text{m}$, respectively. A simple model for internal reflection was taken into account for correction of l_T values.^[38] l_T determined through backscattering method does not decay inversely proportional with $[\text{Nps}]$ and these l_T values are several times lower than l_{T0} values. This is an anomalous and seemingly contradictory result. Therefore, other l_T alternative values (l_{T*}) were also determined considering an increase in the effective refractive index (d near to zero) by localization effect. Let us introduce the following conjecture: if the α_{FF0} increases γ_0 times at d

near to zero because each photon interacts a average of γ_0 times with the same particles, atoms or molecules (within the closed loop path), then n_{eff0} must also increase as $n_{eff0} = 1 + \gamma_0(n_{eff} - 1)$ (see sup. Information). Thereby, in order to estimate the internal reflection, the effective refractive indexes for each [Nps] were scaled through the enhanced “absorption” factor $(n_{eff0} = 1 + \gamma_0(n_{eff} - 1))$ (table SI sup. Information). l_{T^*} values for [47, 70, 140 and 280; $\times 10^{10}$ Nps ml⁻¹], determined through the n_{eff0} correction, correspond to 0.86, 0.6, 0.49 and 0.24 μm , respectively. As can be appreciated, both l_T and l_{T^*} , determined by backscattering method (fig.S6, sup. Information), are several times lower than l_{T0} , which represents another interesting result that could be explained by an l_T decrease in depth (d). Consequently, the coherent backscattering cone yields an l_T value averaged by depth. Of course, the calculus of n_{eff0} and the subsequently determined l_{T^*} values may not be strictly correct because just at $d=0$ an additional increase in the effective refractive index would be expected. Notice that, the l_{s0} , l_{T0} and α_{FF0} are average values determined in a region near to $d=0$, not at $d=0$ (interface silica-sample), where these values should increase even more. Additionally, the enhanced factor of coherent backscattering is lower than expected (1.8) for $[\text{Nps}] \geq 140 \times 10^{10}$ Nps ml⁻¹, which could introduce an error in estimating the backscattering cone angle. The l_T decrease in depth could be an additional evidence of localization transition. Various authors have theoretically suggested the l_T decrease in depth^[16,39] at the critical regime of approaching to localization. This fact can be understood by internal reflection of the coherently backscattered photons in the sample input border, which forces the photons path to be longer. Consequently, the likelihood of closed loop path must also be increased. Furthermore, an increase in the closed loop paths must also induce an increase in the effective refractive index at d near to zero (n_{eff0}), which in turn should lead to the internal reflection increasing. The l_T increase for d near to zero would not mean an increase in the physical distance between two successive scattering events; this could be interpreted as an increase in the effective optical pathlength between two

successive scatterings, because the effective refractive index must increase for d near to zero. Of course this effect would be appreciable when the coherently backscattered light (closed loop paths) starts to have an appreciable contribution. Obviously, the influence of internal reflection decreases with depth; however, it should increase as angle of incidence is increased. The above effects can be understood such that the density of localized states must increase in the vicinity of the boundary, which was theoretically predicted by Mirlin in disordered electronic media.^[39, 40] Other perspective about this issue was provided by Ramos and co-workers,^[41] who demonstrated that the presence of a finite barrier in the input border provokes an increase of the quantum interference (localization) in a disordered electronic medium. The slope decrease with depth in the coherent transmission curves (part I) for $[Np] \geq 47 \times 10^{10} \text{ Np ml}^{-1}$ could be a consequence of l_s decrease in depth. The last has an important physical connotation because it would mean that for large d , the effective “absorption” coefficient (α_{FF}) could be even lower than the classical “absorption” coefficient (α_0). This would imply that the photon cloud propagation does not fill completely all the sample volume, which means that for large d , the photons are propagated by specific paths, i.e. like a much further transmission than the mean free path through the sample^[13] and/or a subwavelength light localization.^[42] This means that, only those photons with very specific entry phase (φ) into the scattering medium (position $(x, y, d=0)$) could reach large d , and that at position (x, y, d) such photons would be strongly correlated. However, at different positions $(x, y, d) - (x', y', d)$ in the d plane the photons would be completely uncorrelated (localization). Therefore, for a large enough d , the photon paths would cease to be equally probable. This statistical problem at the mobility edge in a 3D system was addressed for the first time by Altshuler et al.,^[43] who proposed a Poisson law because the paths would be completely uncorrelated.

Propagating experiment

In order to corroborate localization transition, another one experiment has been performed. The intensity structure of a probe beam (He-Ne laser) was measured after propagating a distance $d=1.8\text{mm}$ through the scattering medium. A CCD camera collected the image of intensity profile $I(x, y)$ at the sample output face (figure S4 supp. information). The input probe beam is $<100\ \mu\text{m}$ full-width at half-maximum (FWHM) and is perpendicular to the sample surface. For the five [Nps], the normalized intensity profiles at samples output are displayed in figure 3. As can be observed, the beam intensity structure narrows as the [Nps] is increased. For $14 \times 10^{10}\ \text{Nps ml}^{-1}$, a Gaussian beam profile $e^{-2(r/\sigma)^2}$ is observed, where r is the radial distance of the beam center. However, for $[\text{Nps}] \geq 47 \times 10^{10}\ \text{Nps ml}^{-1}$, the beam profile ceases to be Gaussian, it could be fitted with a $e^{-2(|r|/\sigma)^{1+\nu}}$ function, where $0 < \nu < 1$. For each [FF], the confinement of the beam at the output plane is quantified by the inverse participation ratio $P \equiv [\int I(x, y)^2 dx dy] / [\int I(x, y) dx dy]^2 = \frac{1}{\pi} [\int I(r)^2 dr] / [\int I(r) dr]^2$, which has units of inverse area, and an effective width $\omega_{\text{eff}} = (P)^{-1/2}$. If absorption is negligible, σ in the fitting function $e^{-2(|r|/\sigma)^{1+\nu}}$ must be proportional to ω_{eff} ($\sigma \propto \omega_{\text{eff}}$).

Figure 3f shows the effective width at the samples output and ν value (extracted from fitting), as a function of filling fraction, revealing that ω_{eff} and ν decrease monotonically as the filling fraction is increased. Notice that for $[280 \times 10^{10}\ \text{Nps ml}^{-1}]$ (fig. 3e), the intensity profile shows a rounding at r near to zero, and for larger r , it decreases more quickly than the $e^{-2(|r|/\sigma)^{1+\nu}}$ fitting function (red solid line). This effect can be associated to an increase in the losses by enhanced “absorption”. In this fitting, ν was fixed and its value was taken by extrapolation (~ 0.28). σ value was also fixed following the same ($\sigma \propto \omega_{\text{eff}}$) criterion. Figure 3g shows the corresponding value of the inverse participation ratio (P) as a function of the filling fraction, along with its statistical standard deviation (marked by error bars). The

statistical standard deviation (ΔP) is determined by $\left(\frac{1}{\pi} \sqrt{\left(\frac{d[P(r)]}{dr}\right)^2} \times \right.$
 $\left. \text{unitdistance}\right)$ evaluated in $r \approx 0$. Figure 3h presents the relative fluctuations of the inverse participation ratio, $\Delta P/P$, as a function of filling fraction. As can be observed, $\Delta P/P$ value increases with the filling fraction. For a filling fraction of 3.5 %, equivalent to $47 \times 10^{10} \text{ Np ml}^{-1}$, $\Delta P/P = 0.67 \cong 2/3$, which corresponds to the onset of localization suggested by Genack and co-workers.^[19] The $\Delta P/P$ increase agrees with the prediction^[16,39] that the relative fluctuations in P are inversely proportional to the dimensionless diffusion coefficient, which must tend to unity (“absorption” negligible) when the system approaches to localization (Poisson law). For $[280 \times 10^{10} \text{ Nps ml}^{-1}]$, $\Delta P/P$ is lightly above unity, which must be a consequence of “absorption”.^[19] The above result represents an additional evidence of localization transition. However, the “absorption” could also have influence over the beam propagation. But, there is not an easy analytical expression for the dependence of “absorption” with angle at the localization transition regime. One can think that the “absorbed” light would increase with r because the effective photon pathlength increases with r . However, the “absorbed” light could increase even more with r at localization transition because the enhanced “absorption” factor can increase with the incidence angle. Notice that, the incidence angle should influence over the photons transport at localization transition because the internal reflection must increase as incidence angle is increased regarding to normal incidence. This fact might increase the likelihood of closed loop paths, leading to a conductance decrease. Therefore, an additional experiment was performed in order to confirm localization transition. The probe beam was introduced in the scattering medium at 30° , 45° and 60° regarding to normal incidence. The intensity profiles $I(x, y)$ at the sample output face were collected for $[\text{Nps}]$ of: 14 and $140 \times 10^{10} \text{ Nps ml}^{-1}$. If ω_{eff} decrease in $[\text{Nps}]$ would be caused by the “absorption”, ω_{eff} must be

independent to incident angle for the two [Nps]. Instead, if ω_{eff} decrease is basically a consequence of the approaching to localization, the profile width should decrease as incidence angle is increased, i.e. a narrowing of the intensity profile must be observed. Notice that an increase in the incidence angle must provoke an increase in the internal reflection of the coherently backscattered photons, i.e. an increase in the effective barrier at the input border. Consequently, an increase in localization must be expected.^[41] This would mean a decrease of diffusion coefficient with incidence angle. This effect would be strong evidence of the approaching to localization, since incidence angle should not be an influence on the “absorption” or in the light transport at diffusive regime. Figures 4a-b show a comparison of the normalized intensity profiles for [14 and 140; $\times 10^{10}$ Nps ml⁻¹] and incidence angles of 0° and 60°. As can be clearly observed for [14 $\times 10^{10}$ Np ml⁻¹] (diffusive regime), the incidence angle has no influence on the intensity profile. However, a narrowing of the intensity profile is observed for [140 $\times 10^{10}$ Np ml⁻¹] (localization transition) as incidence angle is increased, revealing a linear ω_{eff} decrease (fig. 4c). This is strong evidence of an anomalous transport. Note that for the incidence angle of 60° and [140 $\times 10^{10}$ Nps ml⁻¹] (fig. 4b), the intensity profile is sharpened at r near to zero. This could be caused by a decrease of diffusion coefficient. Additionally, the intensity profile decreases more quickly than the fitting function $e^{-2(|r|/\sigma)^{1+\nu}}$ at large r (red solid line). The last could be a consequence of the increase of enhanced “absorption” factor (γ_0) with incidence angle, which must be caused by an increase in the likelihood of closed loop paths by the internal reflection. On the other hand, the narrowing of the intensity profile, as angle of incidence is increased, would be further evidence that the “absorption” effect is negligible for [Nps] $\leq 140 \times 10^{10}$ Np ml⁻¹; such as was inferred from the propagation experiments and total transmission. An expanded study of propagation and “absorption” as a function of incidence angle and [Nps] is called for, in order to understand in depth the photons transport at localization and the associated phenomena to

it. From the above results, a clear transition is observed for $[Nps] \geq 47 \times 10^{10} \text{Nps ml}^{-1}$, which corresponds with a $kl_{T*} \approx 8.6$. This critical value is higher than that reported by Sperling et al. ($kl_T \approx 4.5$).^[10] Note that for $[47 \times 10^{10} \text{Nps ml}^{-1}]$, the filling fraction is only 3.5%. In turn, the critical regime is reached for a filling fraction ~ 10 times lower than that reported by Sperling et al. The higher filling fraction in their samples combined with the high powers used in their experiments must lead to an increase in the inelastic scattering processes.^[11]
^{44]} Probably for this reason, they did not observe an appreciable change in the statistical distribution of the photon cloud. The losses by inelastic scattering must provoke a smoothing in the maximum of intensity profile, appearing like a Gaussian distribution. Additionally, a high filling fraction combined with very high power should also give rise a significant increase in the nonlinear refractive index, leading to an increasing of the photon-photon interaction.^[45] The latter must lead to a decrease in the coherence length, ξ_{coh} . Consequently, a higher scattering strength would be required in order to get the critical regimen of localization transition.

Conclusion

Core-shell $\text{TiO}_2@$ Silica nanoparticles with an appropriate silica shell (thickness and homogeneity) allowed us to obtain a liquid suspension with a significantly high scattering strength. We report several evidences of the critical regime of localization transition in a colloidal suspension, which is achieved at $[Nps] \geq 47 \times 10^{10} \text{Nps ml}^{-1}$. For $[Nps] \geq 47 \times 10^{10} \text{Nps ml}^{-1}$: The transmitted ballistic intensity starts to decay more quickly than an exponential, the “absorption” coefficient (near to zero) shows an quadratic increase in $[Nps]$ (instead a constant value), from which an increase of refractive index also close to zero is proposed; the transmission coefficient starts to show a quadratic decay and a Gaussian probe beam that is propagated through the samples showed a $e^{-2(|r|/\sigma)^{1+\nu}}$ ($0 < \nu < 1$) intensity profile at sample output, instead a Gaussian profile. We also must highlight that for a probe beam inclined

regarding to normal incidence, the intensity profiles are similar for [$14 \times 10^{10} \text{Np ml}^{-1}$] (diffusive regime). However, for [$140 \times 10^{10} \text{Np ml}^{-1}$], a narrowing of the intensity profile is observed as incidence angle is increased. Additionally, an I_T decrease in depth for [$\text{Nps} \geq 47 \times 10^{10} \text{Nps ml}^{-1}$] is inferred from the measurements of coherent backscattering and ballistic transmission (part I).

Acknowledgements

We gratefully acknowledge financial support from FACEPE, CNPq, PRONEX, and to Inomat (INCT de Materiais Complexos Funcionais) for TEM analyses. I.F.S and V.M. thank the CAPES (Brazil) for the fellowships of masters and doctoral, respectively. We extend additional thanks to Professors Luis Poveda, Robin Kaiser, Maurizio Ferrari, Jorge Gabriel, by discussion and their thoughtful suggestions. We appreciate useful experimental support of Dr. Weliton Martins and Dr. Gabriel Basso. Thanks to Engineer Colin Roxburgh, for his corrections to the text.

Author Contributions

All authors conceived, designed, performed and analyzed the experiments; E.J-V, P.C.O, W.M.F. and G.F. de S. contributed materials/analysis tools; E.J-V guided the research and wrote the manuscript.

Additional Information

The authors declare no competing financial interests. Correspondence and requests for materials should be addressed to E.J-V. (Ernesto.Jimenez@uv.es)

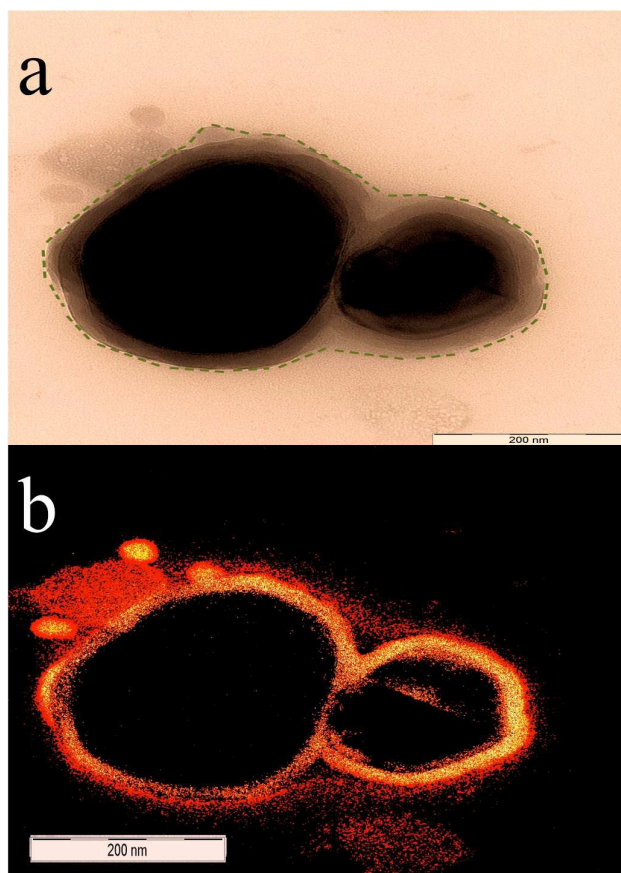


Figure 1. Characterization of TiO₂@Silica nanoparticles via transmission electron microscope. a) TEM image and b) EELS-TEM (Si) chemical mapping of core-shell TiO₂@Silica Nps demonstrates the presence of silicon (orange) onto the TiO₂ surface. The dotted green line (a) indicates the outer surface of the silica coating. The scale bar corresponds to 200 nm.

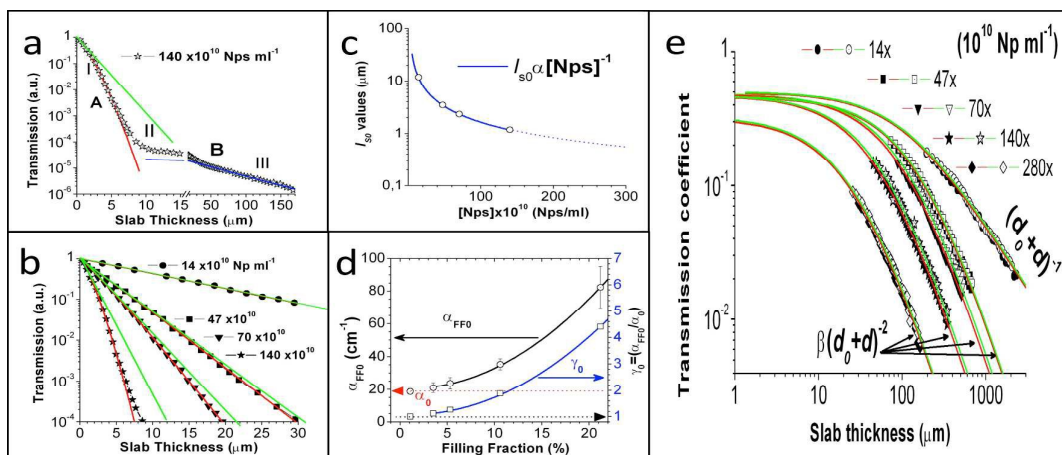


Figure 2. Transport experiments. a) Transmitted coherent intensity (I_{TC}) versus slab thickness [140×10^{10} Nps/ml] (blue line, fitting at part III), and b) I_{TC} for [Nps]: 14, 47, 70, and 140; $\times 10^{10}$ Nps ml^{-1} . The red and green lines represent the decay behavior of experimental points and the exponential fitting with the first experimental points, respectively. c) l_{s0} versus [Nps], d) anomalous increase of: α_{FF0} (left) and the γ_0 (right) as [FF] is increased, red dotted line represents α_0 value, error bars correspond to fitting errors. e) Transmission coefficient for the lasers: pulsed Nd:Yag and CW He-Ne and [Nps] of: 14, 47, 70, 140 and 280; $\times 10^{10}$ Nps ml^{-1} . Open and filled symbols correspond to experimental points for Nd:Yag and He-Ne (lasers), respectively. The green and red solid lines represent the fitting with experimental points for Nd:Yag and He-Ne (lasers), respectively.

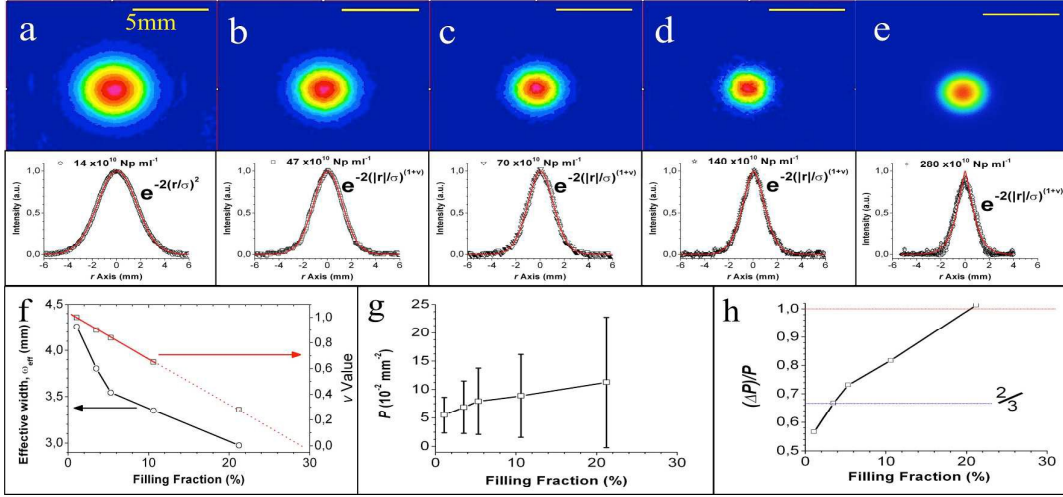


Figure 3. Experimentally measured intensity distributions at the samples output for [Nps]: a) 14 , b) 47 , c) 70 , d) 140 and e) 280 ; $\times 10^{10} \text{ Nps ml}^{-1}$. The propagation length of probe beam was 1.8 mm and scale bar represents 5 mm . For $[14 \times 10^{10} \text{ Np ml}^{-1}]$, the intensity profile fits very well with a gaussian profile $e^{-2(r/\sigma)^2}$. In b), c), d) and e) ($[\text{Nps}] \geq 47 \times 10^{10} \text{ Np ml}^{-1}$), the intensity profiles could be fitted to $e^{-2(|r|/\sigma)^{1+\nu}}$, where $0 < \nu < 1$. f) ω_{eff} (left) and ν (right, red) versus [FF]. g) Inverse participation ratio P as function of [FF]. The error bars are the statistical standard deviations of P ($\Delta P = \left\langle \frac{1}{\pi} \sqrt{\left(\frac{\partial P(r)}{\partial r}\right)^2} (\text{unit distance}) \right\rangle$ around $r = 0$). h) Relative fluctuations of the inverse participation ratio, $(\Delta P/P)$, as a function of [FF]. The increase monotonically of $(\Delta P/P) > 2/3$, and the transition from the gaussian curve of a) to the $e^{-2(|r|/\sigma)^{1+\nu}}$ decaying curves of b), c), d) and e) display the crossover from diffusive transport a) to the localization transition regime.

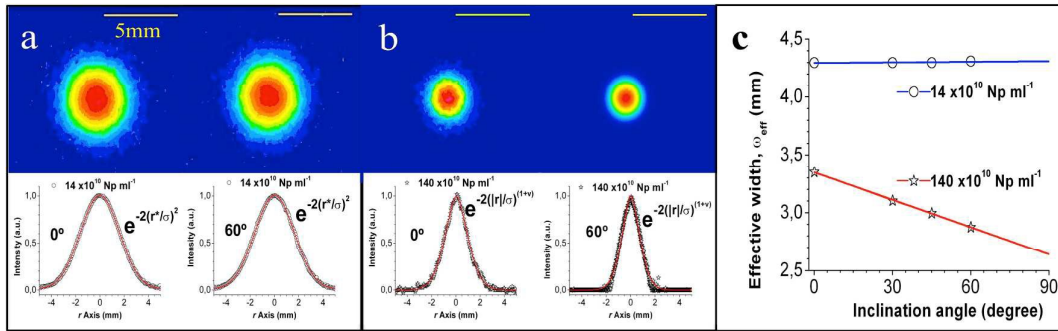


Figure 4. Propagating experiment as a function of incidence angle for: a) $[14 \times 10^{10} \text{ Np ml}^{-1}]$, the output intensity profiles independent to incidence angle, equal Gaussian profiles $e^{-2(r'/\sigma)^2}$ are observed; b) $[140 \times 10^{10} \text{ Np ml}^{-1}]$, the intensity profile narrows as incidence angle is increased, showing a decrease in the photon conductance. c) ω_{eff} monotonically decreases with incidence angle for $[140 \times 10^{10} \text{ Np ml}^{-1}]$, showing that photon transport is determined by localization phenomenon, not by “absorption”, as already was previously inferred.

References

- ¹Wang, H. *et al.* Single-crystalline rutile TiO₂ hollow spheres: room-temperature synthesis, tailored visible-light-extinction, and effective scattering layer for quantum dot-sensitized solar cells. *J. Am. Chem. Soc.* **133**, 19102-19109 (2011).
- ²Vynck, K., Burrese, M., Riboli, F. & Wiersma, D. S. Photon management in two-dimensional disordered media. *Nature Materials* **11**, 1017-1022 (2012).
- ³Cernuto, G., Masciocchi, N., Cervellino, A., Colonna, G. M. & Guagliardi, A. Size and shape dependence of the photocatalytic activity of TiO₂ nanocrystals: a total scattering Debye function study. *J. Am. Chem. Soc.* **133**, 3114-3119 (2011).
- ⁴Andreasen, J. *et al.* Modes of random lasers. *Advances in Optics and Photonics* **3**, 88-127 (2011).
- ⁵Soljacic, M. & Joannopoulos, J. D. Enhancement of nonlinear effects using photonic crystals. *Nature Materials* **3**, 211-219 (2004).
- ⁶Yang, T., Chen, H., Luo, X. & Ma, H. Superscatterer: enhancement of scattering with complementary media. *Optics Express* **16**, 18545-18550 (2008).
- ⁷Sajeev J. Electromagnetic absorption in a disordered medium near a photon mobility edge. *Phys. Rev. Lett.* **53**, 2169 (1984).
- ⁸Wiersma, D. S., Bartolini, P., Lagendijk, A. & Righini, R. Localization of light in a disordered medium. *Nature* **390**, 671-673 (1997).
- ⁹Störzer, M., Gross, P., Aegerter, C. M. & Maret, G. Observation of the critical regime near Anderson localization of light. *Phys. Rev. Lett.* **96**, 063904 (2006).
- ¹⁰Sperling, T., Bührer, W., Aegerter, C. M. & Maret, G. Direct determination of the transition to localization of light in three dimensions. *Nature Photon.* **7**, 48-52 (2013).
- ¹¹Sperling, T., Bührer, W., Ackermann, M., Aegerter, C. M. & Maret, G. Probing Anderson localization of light by weak non-linear effects. *New Journal of Physics* **16**,

112001 (2014).

¹²vanAlbada M. P. & Lagendijk, A. Observation of weak localization of light in a random medium. *Phys. Rev. Lett.* **55**, 2692 (1985).

¹³Vellekoop, I. M. & Mosk, A. P. Focusing coherent light through opaque strongly scattering media. *Opt. Lett.* **32**, 2309 (2007).

¹⁴Chong, Y. D. & Stone, A. D. Hidden Black: Coherent Enhancement of Absorption in Strongly Scattering Media. *Phys. Rev. Lett.* **107**, 163901 (2011).

¹⁵Ioffe, A.F. & Regel, A. R. Non-crystalline, amorphous and liquid electronic semiconductors. *Progr. Semiconductors* **4**, 237-291 (1960).

¹⁶Abrahams, E., Anderson, P. W., Licciardello, D. C. & Ramakrishnan, T. V. Scaling Theory of Localization: Absence of Quantum Diffusion in Two Dimensions. *Phys. Rev. Lett.* **42**, 673–676 (1979).

¹⁷Anderson, P. W. The question of classical localization A theory of white paint? *Phil. Mag.* **B52**, 505–509 (1985).

¹⁸Scheffold, F., Lenke, R., Tweert, R. & Maret, G. Localization or classical diffusion of light? *Nature* **398**, 206 (1999).

¹⁹Chabanov, A. A., Stoytchev, M. & Genack, A. Z. Statistical signatures of photon localization. *Nature* **404**, 850 (2000).

²⁰van der Beek, T., Barthelemy, P., Johnson, P. M., Wiersma, D. S. & Lagendijk, A. Light transport through disordered layers of dense gallium arsenide submicron particles. *Physical Review* **B85**, 115401 (2012).

²¹Jimenez-Villar, E., Mestre, V., Oliveira, P. C. & de Sá, G. F. Novel core-shell (TiO₂@Silica) nanoparticles for scattering medium in a random laser: higher efficiency, lower laser threshold and lower photodegradation. *Nanoscale* **5**, 12512-12517 (2013).

²²Jimenez-Villar, E. et al. TiO₂@Silica nanoparticles in a random laser: Strong

relationship of silica shell thickness on scattering medium properties and random laser performance. *Appl. Phys. Lett.* **104**, 081909(2014).

²³Rodriguez, E. et al. Fabrication and characterization of a PbTe quantum dots multilayer structure. *Physica E* **26**, 361(2005).

²⁴Rodriguez, E., Kellerman, G., Jiménez, E., César, C.L. & Barbosa, L.C., *Superlattices and Microstructures* **43**, 626-634 (2008).

²⁵ Jimenez, E., Abderrafi, K., Abargues, R., Valdes, J. L. & Martinez-Pastor, J., Laser-ablation-induced synthesis of SiO₂-capped noble metal nanoparticles in a single step. *Langmuir* **26**, 7458-7463(2010).

²⁶Jimenez, E., Abderrafi, K., Martinez-Pastor, J., Abargues, R., Valdes, J.L., Ibañez, R., *Superlattices and Microstructures* **43**, 487–493 (2008).

²⁷Gonzalez-Castillo J. R. et al. Synthesis of Ag@Silica nanoparticles by assisted laser ablation. *Nanoscale Research Letters* **10**:399 (2015).

²⁸ Fuertes, G. et al. Switchable bactericidal effects from novel silica-coated silver nanoparticles mediated by light irradiation. *Langmuir* **27**, 2826-2833(2011).

²⁹Rodríguez, E., Jimenez, E., Neves, A.A.R., Padilha, L.A., Jacob, G.J., Cesar, C.L., Barbosa, L.C. *Appl. Phys. Lett.* **2005**, 86, 113117.

³⁰ Kellermann, G. et al. Structure of PbTe(SiO₂)/SiO₂ multilayers deposited on Si(111). *Journal of Applied Crystallography* **43**, 385-393(2010).

³¹Demiroors, A. F., Blaaderen, A. V. & Imhof, A. Synthesis of eccentric titania–silica core–shell and composite particles. *Chem. Mater.* **21**, 979-984 (2009).

³²Abderrafi, K., Jimenez, E., Ben, T., Molina, S.I., Ibañez, R., Chirvony, V., Martínez-Pastor, J. *Journal of Nanoscience and Nanotechnology* **2012**, 12, 6774-6778.

-
- ³³Karmakar, B., De, G. &Ganguli, D. Dense silica microspheres from organic and inorganic acid hydrolysis of TEOS. *Journal of Non-Crystalline Solids***272**, 119-126 (2000).
- ³⁴Jimenez-Villar, E. et al. Random lasing at localization transition in a colloidal suspension (TiO₂@Silica), **unpublished**.
- ³⁵Sajeev J. Localization of light. *Physics Today***44**, 32 (1991).
- ³⁶Smaranda I. et al. “Abnormal anti-Stokes Raman scattering and coherent backscattering as manifestation of Anderson localization of light in nonlinear mesoscopic materials; *Optical Engineering***53(9)**, 097109 (2014).
- ³⁷Campagnano, G. &Nazarov Yu. V. G_0 corrections in the circuit theory of quantum transport. *Physical Review B***74**, 125307 (2006).
- ³⁸Legendijk, A., Vreeker, R. & de Vries, P. Influence of internal reflection on diffusive transport in strongly scattering medium. *Physics Letters A***1989**, Vol. **136 (1-2)**, 81-88.
- ³⁹ Mirlin, A. D. Statistics of energy levels and eigenfunctions in disordered systems. *Physics Reports***326**, 259-382(2000).
- ⁴⁰Mirlin, A.D. Spatial structure of anomalously localized states in disordered conductors. *J. Math. Phys.***38**, 1888 (1997).
- ⁴¹Barbosa, A.L.R., Bazeia, D. & Ramos J.G.G.S. Universal Braess paradox in open quantum dots. *Physical Review E* **90**, 042915 (2014).
- ⁴² Molinari, D. & Fratalocchi, A. Route to strong localization of light: the role of disorder. *Optical Express***20**, 18156 (2012).
- ⁴³Altshuler, B.L., Zharekeshev, I.Kh., Kotochigova, S.A. & Shklovskii, B.I. Repulsion between energy levels and the metal-insulator transition. *Zh. Eksp. Teor. Fiz.***94**, 343 (1988) [*Sov. Phys. JETP***67**, 625 (1988)].

⁴⁴Bührer, W. Anderson Localization of Light in the Presence of Non-linear Effects. PhD thesis, Univ. Konstanz (2012).

⁴⁵ Bromberg, Y., Lahini, Y., Small E. & Silberberg, Y. Hanbury Brown and Twiss interferometry with interacting photons. *Nature photonics* **4**, 721-726 (2010).